

# Lignin Valorization by Forming Toughened Thermally Stimulated Shape Memory Copolymeric Elastomers: Evaluation of Different Fractionated Industrial Lignins

Hui Li, Gopakumar Sivasankarapillai, Armando G. McDonald

Renewable Materials Program, Department of Forest, Rangeland, and Fire Sciences, University of Idaho, Moscow, Idaho 83844-1132

Correspondence to: A. G. McDonald (E-mail: armandm@uidaho.edu)

**ABSTRACT:** Lignin-based thermal responsive dual shape memory copolymeric elastomers were prepared with a highly branched pre-polymer (HBP, A<sub>2</sub>B<sub>3</sub> type) via a simple one-pot bulk polycondensation reaction. The effect of fractionated lignin type (with good miscibility in the HBP) on copolymer properties was investigated. The thermal and mechanical properties of the copolymers were characterized by DMA, DSC, and TGA. Tensile properties were dominated by HBP <45% lignin content while lignin dominated >45% content. The copolymers glass transition temperature ( $T_g$ ) increased with lignin content and lignin type did not play a significant role. Thermally stimulated dual shape memory effects (SME) of the copolymers were quantified by cyclic thermomechanical tests. All copolymers had shape fixity rate >95% and >90% shape recovery for all compositions. The copolymer shape memory transition temperature ( $T_{trans}$ ) increased with lignin content and  $T_{trans}$  was 20°C higher than  $T_g$ . Lignin, a renewable resource, can be used as a netpoint segment in polymer systems with SME behavior. © 2014 Wiley Periodicals, Inc. *J. Appl. Polym. Sci.* **2015**, *132*, 41389.

**KEYWORDS:** biopolymers & renewable polymers; dendrimers; elastomers; hyperbranched polymers and macrocycles; stimuli-sensitive polymers

Received 9 April 2014; accepted 12 August 2014

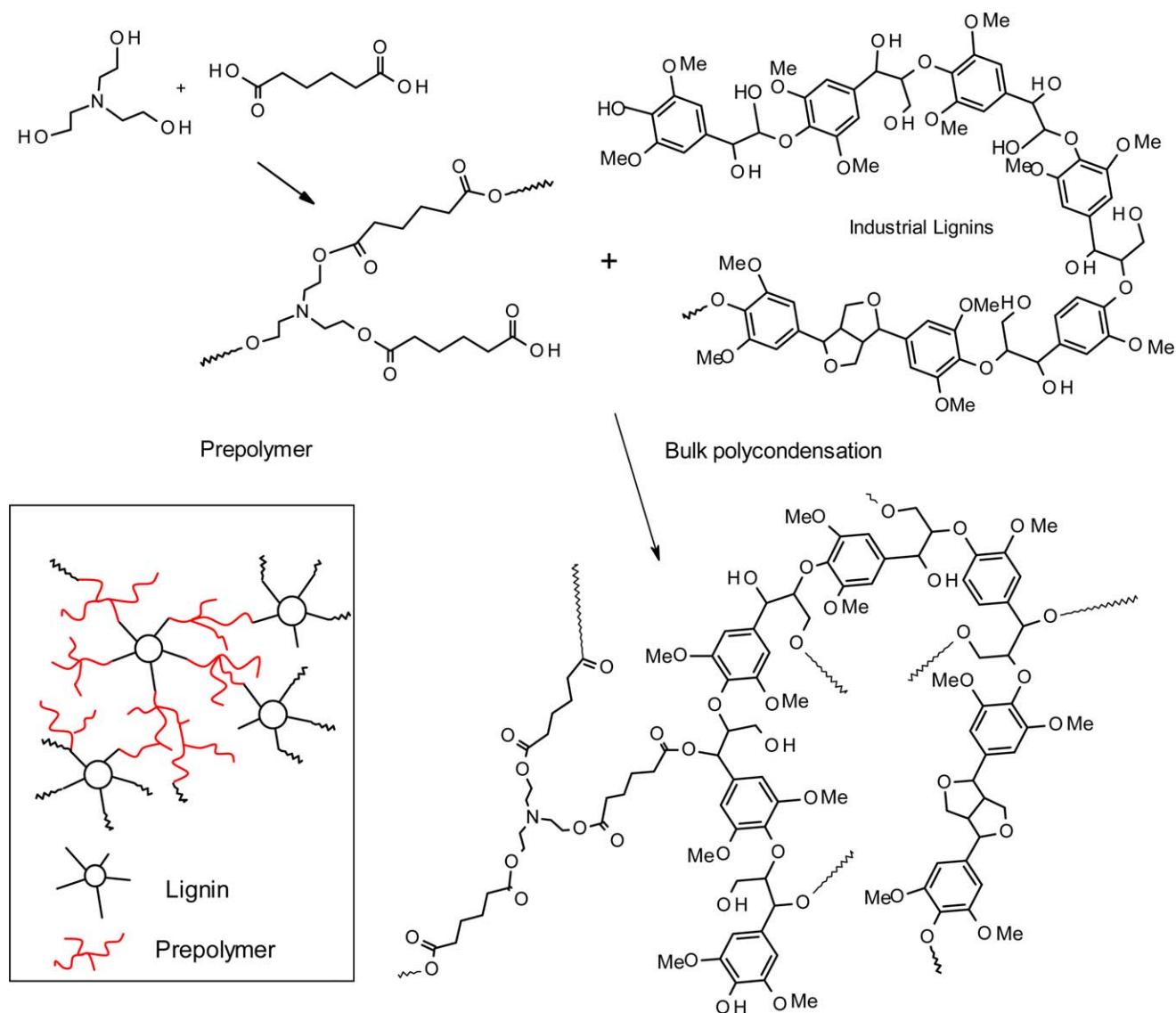
DOI: 10.1002/app.41389

## INTRODUCTION

Petroleum-based polymers are important materials and used extensively in modern society. The United States alone produced  $4.7 \times 10^{10}$  kg of all polymers during 2010.<sup>1</sup> However, these are derived from non-renewable resources and have a large carbon foot print.<sup>2</sup> Alternatively, the utilization of bio-resources to produce sustainable bio-based materials can overcome the finite petroleum resource and offset CO<sub>2</sub> emissions. Currently, considerable efforts have been made in the development of commercial biopolymers fabricated from refined natural resources (e.g. glucose) including poly(lactic acid),<sup>3–6</sup> cellulose derivatives,<sup>7,8</sup> polyhydroxyalkanoate (poly(hydroxybutyrate),<sup>9</sup> poly(2-hydroxybutyrate-co-hydroxyvalerate)),<sup>10</sup> thermoplastic starch<sup>11,12</sup> and vegetable-oil-based polymers.<sup>13–15</sup> However, there is potential to produce biopolymers from industrial byproduct streams, such as lignin from cellulosic ethanol or pulping operations.

Lignin is an underdeveloped feedstock for producing polymers. Lignin is distributed widely throughout the plant kingdom and its abundance is behind that of cellulose and hemicellulose (15–30% by weight).<sup>16,17</sup> However, lignin is historically treated as byproduct of pulp and paper industry which produced substan-

tial amounts of industrial lignin, for example,  $4.5 \times 10^{10}$  kg in 2004.<sup>18</sup> Merely 2% of industrial lignin is commercialized into low-value products such as dispersing or binding agents with remainder burned as compensating fuel.<sup>19</sup> Possible reasons for its low utilization is its brittleness and high glass transition temperature ( $T_g$ ) due to lignin's rigid aromatic backbone and inter/intra-molecular H-bonding structures.<sup>20</sup> To improve lignin's properties, solvent partitioning has been successfully employed to obtain a fraction of low molar mass and  $T_g$  as well as good miscibility with other polymers.<sup>21</sup> Furthermore, the chemical structural variations due to species and extraction techniques can result in large heterogeneity within lignin. Therefore, modification of lignin mainly focused on reducing the H-bonding by substitution resulting in lowering the  $T_g$  and improving its toughness and flexibility. Chemical modification approaches employed to alleviate the situation are alkylation (similar to polystyrene in terms of tensile properties),<sup>22</sup> benzylation (tunable  $T_g$  as degree of substitution varied from 183°C to 60°C),<sup>23</sup> oxypropylation (obtained polyols with decreased  $T_g$  and for polyurethane fabrications),<sup>24–27</sup> and esterification.<sup>28,29</sup> Esterification is probably the most feasible pathway to carry out in terms of the reaction parameters and reactants. Other lignin based



### Lignin-highly branched poly(ester-amine) polymeric systems

**Scheme 1.** Synthetic route for lignin-copoly(ester-amine) elastomer. [Color figure can be viewed in the online issue, which is available at [wileyonlinelibrary.com](http://wileyonlinelibrary.com).]

polymers products incorporate polyester, epoxy resins, xylic acid-polyurethane and elastomeric materials.<sup>21,30–34</sup> A comprehensive review on lignin chemical modification could be found in a recent report by Laurichesse and Avérous.<sup>35</sup> Furthermore, lignin based thermoresponsive materials were obtained which transited from hydrophilic to hydrophobic nature above 32°C in aqueous solution.<sup>36</sup>

Polymers that have the ability to memorize different shapes and can be recovered in a predefined way upon exertion of suitable stimulus such as heat, magnetism, electricity, moisture, or light, are designated as shape memory polymers (SMPs).<sup>37–45</sup> Temperature caused shape change is named thermally stimulated shape memory effect (Ts-SME).<sup>37</sup> Since SMPs were first introduced 1984 in Japan,<sup>46</sup> they have attracted increasing attentions both

in academic and industrial fields and been used in smart fabrics, heat shrinkable tubes for electronics, films for packaging, self-deployable sun sails in spacecraft, self-disassembling mobile phones, intelligent medical devices, and implants for minimally invasive surgery.<sup>39</sup> In principle, a SMP is first heated to a deformation temperature ( $T_d$ ), which leads to the material softening (storage modulus ( $E$ ) drop). A deformation force is subsequently applied (i.e. loading, strain controlled or stress controlled).<sup>47</sup> The SMP is then cooled down to lower temperature still under load. The deformed shape is then fixed before removal of load. The programming is the procedure of the shape fixing. When the deformed SMP under temporary shape is re-heated to a higher temperature without stress exertion, the permanent shape is recovered. Typically both deformation temperature and so-called recovery temperature are above the

**Table I.** Aromatic/Aliphatic Hydroxyl Group Ratio Determination from Acetylated Lignin by FT-IR and <sup>1</sup>H NMR

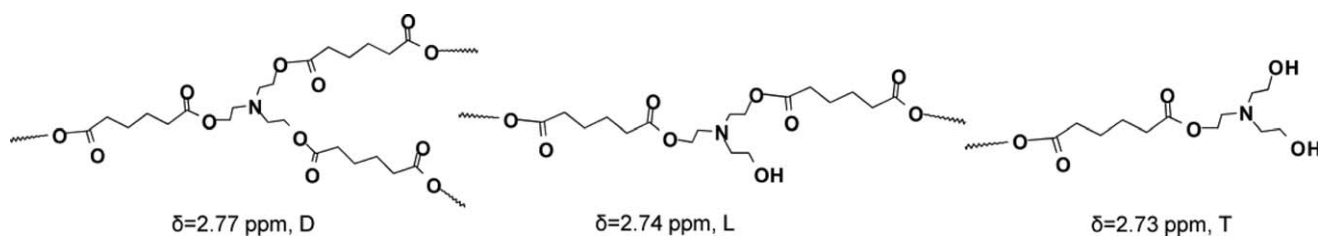
Lignin	Aromatic/Aliphatic OH	
	FT-IR	<sup>1</sup> H NMR
IN	1.05	1.01
PB	0.93	0.93
CS	1.07	1.07

**Table II.** Molar Mass Determination of Different Fractionated Industrial Lignins and E1 Prepolymer

Sample	IN	PB	CS	E1
<i>M<sub>n</sub></i> (g/mol)	355	658	446	987
<i>M<sub>w</sub></i> (g/mol)	654	958	741	1206
PDI	1.84	1.46	1.66	1.22

reversible thermal transition temperature ( $T_g$  or melting point  $T_m$ ) of the SMP, which is thus called shape memory transition ( $T_{trans}$ ).<sup>44</sup> Ts-SME could not be simply obtained via single polymers, but a combination of polymer structures or polymer morphologies with in turn distinct  $T_g$ s, where two segments are responsible for the Ts-SME, netpoints segment (controlling permanent shape, sometimes also called hard segment) and switching segment (controlling temporary shape, also called soft segment). Liu et al.<sup>41</sup> comprehensively reviewed four classes of SMPs based on molecular architectures, that is, chemically cross-linked glassy thermosets; chemically cross-linked semi-crystalline rubbers; physically cross-linked thermoplastics; and physically cross-linked block copolymers.

This current investigation belongs to the chemically cross-linked glassy thermoset mechanism, where  $T_{trans}$  is controlled by  $T_g$ . Our previous research developed protocols for the synthesis and characterization of lignin based elastomeric copolymers with highly branched prepolymer (HBP)<sup>21,31</sup> and partially cross-linked long alkyl chain HBP.<sup>32</sup> Lignin was the rigid “netpoint” segment with high  $T_g$  while the HBP was the soft highly flexible segment with appreciably low  $T_g$ . Therefore, we hypothesize that the copolymer of lignin and HBP would possess Ts-SME. Based on the hypothesis, copolymers from lignin and HBP were synthesized and investigated with respects to determining their SME properties. Furthermore, different fractionated industrial lignins and content were evaluated in order to tailor their thermal, mechanical, and SME properties.

**Scheme 2.** Branching structures in E1 prepolymer; Dendritic (D), linear (L) and terminal (T).

## MATERIALS AND METHODS

### Materials

Indulin AT softwood kraft lignin (MeadWestvaco), Protobind 1000 soda lignin (ALM India Pvt. Ltd.), and corn stover lignin (CS, National Renewable Energy Laboratory) were used. Corn stover lignin was washed with hot water and freeze dried. Each lignin (250 g) type was fractionated by stirring in methanol (1500 mL) for 5 h at 50°C and the methanol soluble fraction was filtered, concentrated to dryness and yields recorded.<sup>48</sup> The methanol soluble lignin yields for protobind, indulin and corn stover were 50%, 45%, and 12%, respectively. These methanol soluble lignins (respectively coded PB, IN, and CS) were used for copolymer synthesis; 1,1,1-triethanolamine (TEA, B<sub>3</sub>), adipic acid (AA, A<sub>2</sub>), methanol and tetrahydrofuran (THF) were obtained from Acros Organics and used as received.

### Methods

**Synthesis of HBP Poly(ester-amine) (E1).** The synthetic method was described in our previous publication.<sup>31</sup> The mixture of TEA (0.04 mol) and AA (0.08 mol) with mole ratio 1 : 2 was prepared in a beaker (50 mm dia), then the beaker was placed in a preheated vacuum oven. The polycondensation reaction was controlled to below 650 mmHg at 100°C. The reaction was monitored every 2 h to check the reaction viscosity and solubility in methanol.

Yield: 94%; IR (ATR, cm<sup>-1</sup>):  $\nu = 3500\text{--}3200$  (vb;  $\nu(\text{OH stretching})$ ), 2945 (s;  $\nu_{as}(\text{CH}_2)$ ), 2870 (s;  $\nu_s(\text{CH}_2)$ ), 2500 (vb; (OH of COOH)), 1723 (vs; (C=O from ester)), 1558 (m; (COO<sup>-</sup>)), 1455 (w, (CH<sub>2</sub>)), 1391 (w; (OH)), 1169 and 1140 cm<sup>-1</sup> (vs; (COO in ester)); <sup>1</sup>H NMR (500 MHz, DMSO-*d*<sub>6</sub>,  $\delta$ ): 4.00–4.06 (m, N-CH<sub>2</sub>-CH<sub>2</sub>-O), 3.39–3.46 (m, N-CH<sub>2</sub>-CH<sub>2</sub>-OH), 2.72–2.79 (m, N-CH<sub>2</sub>-CH<sub>2</sub>-O), 2.56–2.63 (m, N-CH<sub>2</sub>-CH<sub>2</sub>-OH), 2.50 (p, DMSO-*d*<sub>6</sub>), 2.25–2.31 (m, -OOC-CH<sub>2</sub>-CH<sub>2</sub>-), 2.17–2.23 (m, HOOC-CH<sub>2</sub>-CH<sub>2</sub>-), 1.45–1.57 (m, -OOC-CH<sub>2</sub>-CH<sub>2</sub>-CH<sub>2</sub>-CH<sub>2</sub>-COO-); <sup>13</sup>C NMR (125.76 MHz, DMSO-*d*<sub>6</sub>,  $\delta$ ): 174.24 and 174.19 (COOH), 172.61 (COO-), 62.16 and 62.11 (N-CH<sub>2</sub>-CH<sub>2</sub>-O), 59.37, 59.29 and 58.91 (N-CH<sub>2</sub>-CH<sub>2</sub>-OH), 57.00, 56.96, and 56.72 (N-CH<sub>2</sub>-CH<sub>2</sub>-OH), 53.02, 52.87 and 52.64 (N-CH<sub>2</sub>-CH<sub>2</sub>-O), 33.36 and 33.27 (HOOC-CH<sub>2</sub>-CH<sub>2</sub>-), 33.18 and 33.09 (-OOC-CH<sub>2</sub>-CH<sub>2</sub>-), 24.00, 23.90, 23.80 (-OOC-CH<sub>2</sub>-CH<sub>2</sub>-CH<sub>2</sub>-CH<sub>2</sub>-COO-).

**Synthesis of Lignin-Copoly(ester-amine).** Lignin samples (IN, PB, and CS) were dispersed in the minimum amount of THF and mixed with HBP E1 proportionally to synthesize lignin-copoly(ester-amine). THF was then removed under a stream of N<sub>2</sub> at 80°C. The highly viscous mixture was then transferred to a prepared aluminum pan (15 × 15 cm<sup>2</sup>) and was placed into

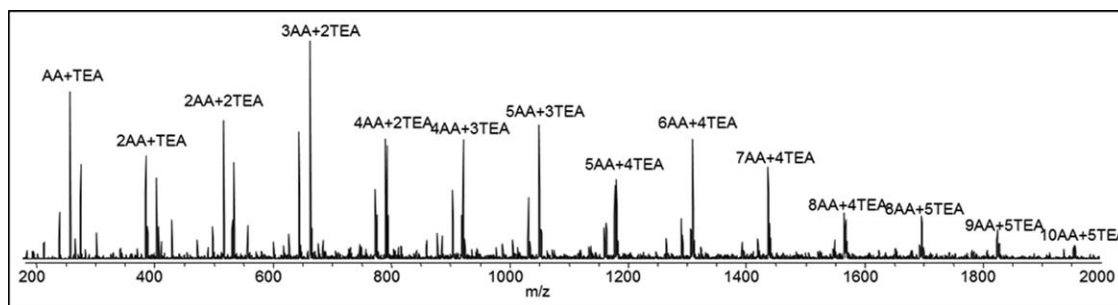


Figure 1. Positive ion distribution of E1 prepolymer from ESI-MS.

vacuum oven at 80°C and 750 mmHg to remove residual solvent and moisture (about 30 min). Then the reaction temperature was increased to 120°C at 650 mmHg, and the reaction proceeded for 20 hrs. The final lignin-copoly(ester-amine) displayed a highly bright and glossy surface and was insoluble in common organic solvents. Copolymers were prepared from the three lignin types at varying lignin contents. The synthesis approach is shown in Scheme 1.

IR (ATR,  $\text{cm}^{-1}$ ):  $\nu = 3500\text{--}3200$  (vb;  $\nu(\text{OH stretching})$ ), 2945 (s;  $\nu_{\text{as}}(\text{CH}_2)$ ), 2870 (s;  $\nu_{\text{s}}(\text{CH}_2)$ ), 1726 (vs; (C=O from ester)), 1600 (m; aromatic skeletal vibration), 1512 (m; aromatic skeletal vibration), 1455 (w,  $(\text{CH}_2)$ ), 1419 (w, CH in-plane deformation), 1378 (w,  $\text{CH}_3$ ), 1169 and 1140  $\text{cm}^{-1}$  (vs; (COO in ester)).

#### Characterization Techniques

**FT-IR and NMR.** All Fourier transform-infrared (FT-IR) spectra were carried out with a Thermo Nicolet Avatar 370 spectrometer operating in the attenuated total reflection (ATR) mode (Smart performance, ZnSe crystal).  $^1\text{H}$  and  $^{13}\text{C}$  nuclear magnetic resonance (NMR) spectra were obtained on prepolymer and acetylated lignin<sup>49</sup> samples on a Bruker Avance 500 spectrometer. Chemical shifts were referenced to DMSO- $d_6$  at 39.5 for  $^{13}\text{C}$  and 2.50 for  $^1\text{H}$  spectra at 30°C.<sup>31</sup>

#### Electrospray Ionization—MS

Molar mass of the lignin and E1 HBP samples were determined by positive ion ESI-MS on a LCQ-Deca instrument (Thermo Finnigan). Lignin samples were dissolved in methanol (1 mg/mL)

containing 1% acetic acid and introduced into the ESI source at a flow rate of 10  $\mu\text{L}/\text{min}$ .<sup>50</sup> The ion source and capillary voltages were 4.48 kV and 47 V, respectively at a temperature of 275°C. The MS were scanned between  $m/z$  (mass to charge ratio) 150 and 2000. The number average molar mass ( $M_n$ ) was calculated as  $M_n = \sum M_i N_i / \sum N_i$  and weight average molar mass ( $M_w$ ) as  $M_w = \sum M_i^2 N_i / \sum M_i N_i$  where  $M_i$  and  $N_i$  are the  $m/z$  and intensity of the ions, respectively.<sup>51</sup>

#### Thermal and Mechanical Analysis

Differential scanning calorimetric (DSC) was performed on a TA instruments model Q200 DSC equipped with a refrigeration cooling unit to monitor the thermal behavior of materials. The polymers (5–7 mg) were analyzed from  $-70^\circ\text{C}$  to  $50^\circ\text{C}$  at a heating rate of  $3^\circ\text{C}/\text{min}$  and held isothermally for 5 min. All the data were collected from the second heating cycle (typically from  $-70$  to  $50^\circ\text{C}$ ). Lignin samples were annealed at  $90^\circ\text{C}$  for 10 min, then cooled to  $0^\circ\text{C}$  (3 min), then heated to  $200^\circ\text{C}$  at  $10^\circ\text{C}/\text{min}$  (second cycle). Thermogravimetric analysis (TGA) was performed on a TGA-7 (Perkin Elmer) instrument from 50 to  $900^\circ\text{C}$  at a heating rate of  $20^\circ\text{C}/\text{min}$  in  $\text{N}_2$ . Dynamic mechanical analysis (DMA) experiments were performed using a TA Instruments model Q800 DMA, both under isothermal and non-isothermal conditions in  $\text{N}_2$  atmosphere in the tensile mode (12 mm  $\times$  4 mm  $\times$  0.2 mm). The heating scans were carried out at 1 Hz and at a heating rate of  $3^\circ\text{C}/\text{min}$ . The tensile properties of the polymeric materials (triplicate per sample) were measured using DMA at room temperature with ramp 3 N/min.

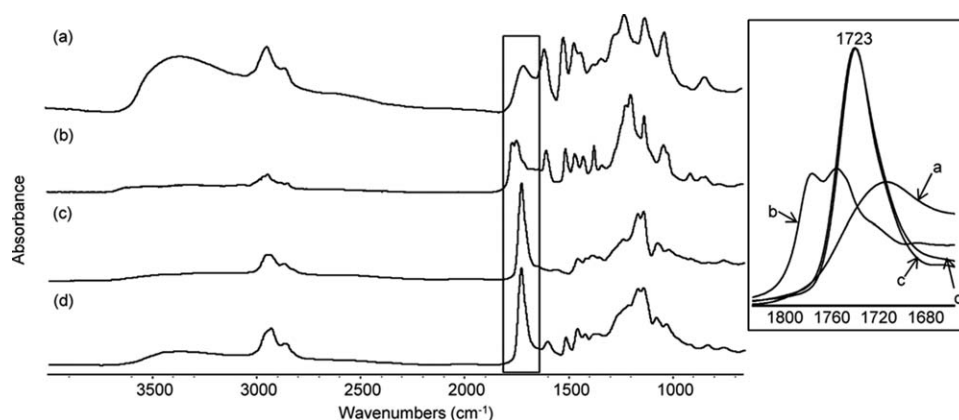


Figure 2. FT-IR spectra of (a) PB, (b) acetylated PB, (c) E1-0 polymer and (d) PBE1-40 copolymer.

**Table III.** ESI-MS Ion Assignments of E1 Oligomeric Structures

m/z	Ion percentage (%)	Composition	m/z	Ion percentage (%)	Composition
260	1.4	[AA + TEA-2H <sub>2</sub> O + H] <sup>+</sup>	1052	6.6	[5AA + 3TEA-7H <sub>2</sub> O + H] <sup>+</sup>
278	5.1	[AA + TEA-H <sub>2</sub> O + H] <sup>+</sup>	1165	2.0	[5AA + 4TEA-9H <sub>2</sub> O + H] <sup>+</sup>
388	5.3	[2AA + TEA-3H <sub>2</sub> O + H] <sup>+</sup>	1183	4.5	[5AA + 4TEA-8H <sub>2</sub> O + H] <sup>+</sup>
406	3.4	[2AA + TEA-2H <sub>2</sub> O + H] <sup>+</sup>	1293	2.0	[6AA + 4TEA-10H <sub>2</sub> O + H] <sup>+</sup>
519	5.1	[2AA + 2TEA-4H <sub>2</sub> O + H] <sup>+</sup>	1311	8.0	[6AA + 4TEA-9H <sub>2</sub> O + H] <sup>+</sup>
537	3.8	[2AA + 2TEA-3H <sub>2</sub> O + H] <sup>+</sup>	1421	1.4	[7AA + 4TEA-11H <sub>2</sub> O + H] <sup>+</sup>
647	4.0	[3AA + 2TEA-5H <sub>2</sub> O + H] <sup>+</sup>	1439	6.9	[7AA + 4TEA-10H <sub>2</sub> O + H] <sup>+</sup>
665	6.8	[3AA + 2TEA-4H <sub>2</sub> O + H] <sup>+</sup>	1567	3.6	[8AA + 4TEA-11H <sub>2</sub> O + H] <sup>+</sup>
775	2.9	[4AA + 2TEA-6H <sub>2</sub> O + H] <sup>+</sup>	1681	0.9	[8AA + 5TEA-13H <sub>2</sub> O + H] <sup>+</sup>
793	6.1	[4AA + 2TEA-5H <sub>2</sub> O + H] <sup>+</sup>	1698	2.8	[8AA + 5TEA-12H <sub>2</sub> O + H] <sup>+</sup>
906	4.5	[4AA + 3TEA-7H <sub>2</sub> O + H] <sup>+</sup>	1826	1.8	[9AA + 5TEA-13H <sub>2</sub> O + H] <sup>+</sup>
924	6.4	[4AA + 3TEA-6H <sub>2</sub> O + H] <sup>+</sup>	1958	0.8	[10AA + 5TEA-14H <sub>2</sub> O + H] <sup>+</sup>
1034	3.8	[5AA + 3TEA-8H <sub>2</sub> O + H] <sup>+</sup>			
General formula			[AA <sub>x</sub> + TEA <sub>y</sub> -H <sub>2</sub> O <sub>z</sub> + H] <sup>+</sup> (z = x + y): cyclic		
			[AA <sub>x</sub> + TEA <sub>y</sub> -H <sub>2</sub> O <sub>a</sub> + H] <sup>+</sup> (a = x + y - 1): acyclic		

The SME of lignin based copolymers were determined in the tensile mode using a DMA. A stress-controlled cycle thermomechanical test was applied. Four programming steps were proceeded, in which (i) the copolymers were heated to a temperature of  $T_g$  ( $E'$  maxima) 20°C (designated as  $T_{high}$ ) with ramp of 5°C/min, then set load to 2 N static force with ramp of 0.2 N/min, the copolymers were stretched to temporary shapes; (ii) cooled to  $T_g - 20^\circ\text{C}$  (ramp 5°C/min) (designated as  $T_{low}$ ); and (iii) release the static force while keeping at  $T_{low}$ , the copolymers kept the temporary shapes; (iv) heated up to  $T_{high}$  again and kept isothermal for 15 mins, the permanent shape was achieved again. The same programming procedure was repeated for three times (cycle 1 to 3).

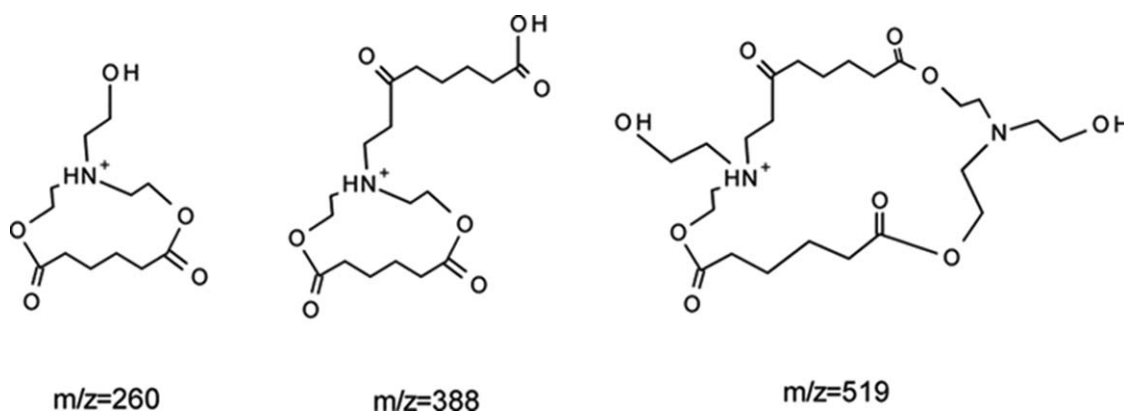
## RESULTS AND DISCUSSION

### Preparation and Analyses of Lignin and HBP Samples

The thermal and chemical properties of starting materials (lignin and HBP) were partially characterized in our previous

research.<sup>31,48</sup> Starting material properties would play an important role in subsequent polymerization. For lignin, the ease of solubility, abundance of hydroxyl groups, molecular mass and  $T_g$ , while for the HBP, the amount of available carboxylic acid groups, chemical branching structure and  $T_g$  are of significance.

The commercial lignin samples were separated into a low molar mass fraction by solubilization in hot methanol. The fractionated lignin samples were measured for lignin content by the Klason lignin plus acid soluble lignin procedures at IN (94.0%), PB (93.3%), and CS (95.4%).<sup>48</sup> Aromatic and aliphatic hydroxyl group contents in lignin, as their acetate, were quantitatively determined by FT-IR (1762  $\text{cm}^{-1}$  (aromatic ester) and 1743  $\text{cm}^{-1}$  (aliphatic ester)) [Figure 2(b)] and <sup>1</sup>H NMR (2.28 ppm (aromatic ester) and 2.01 ppm (aliphatic ester)) techniques (Table I). The two techniques gave similar results, except for IN.  $M_w$  of lignin samples were determined by ESI-MS (Table II). The PB had the highest  $M_w$  at 958 g/mol and the results are consistent with fractionated commercial lignin.<sup>52</sup> To assess the



**Scheme 3.** Possible cyclic structures in E1 prepolymer.

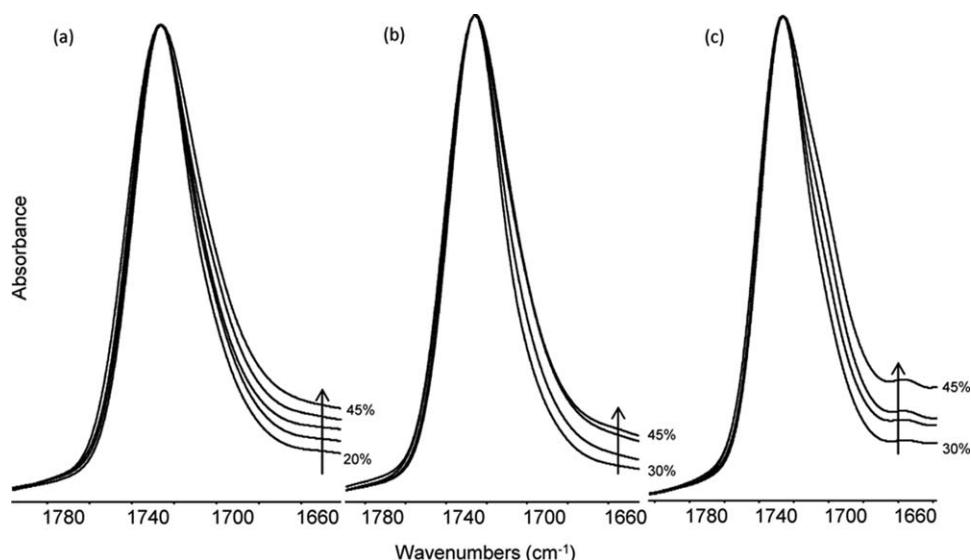


**Figure 3.** FT-IR spectra of the carbonyl region of (a) PBE1-20 to 45 copolymer, (b) INE1-30 to 45 copolymer, and (c) CSE1-30 to 45 copolymer. Note: arrows mean increase in lignin content.

thermal stability of the lignin samples (IN, PB, and CS) during subsequent copolymerization reaction they were exposed to 120°C for 20 h and the  $M_w$  determined by ESI-MS. Only slight increases (about 2%) in lignin  $M_w$  were observed and this suggests that minimal condensation occurred and would not pose a problem during copolymerization. Work by Cui et al. has also shown minimal changes in kraft lignin  $M_w$  when heated at 120°C.<sup>24</sup>

The HBP E1 ( $A_2B_3$ ) was prepared according to our previous procedure<sup>31</sup> with slight modification. In the HBP synthesis, the reaction conditions were controlled to make sure that only partial conversion of functional groups from monomers occurred to prevent the formation of cross-linked or excessively high

molar mass polymers. The resulting polymers were slightly yellow in color and were highly viscous in nature. Ester formation was confirmed by FT-IR ( $1723\text{ cm}^{-1}$ ) and  $^{13}\text{C}$  NMR (172.6 ppm). The carboxylic acid group (174 ppm) in E1 and hydroxyl group ( $\sim 3500\text{ cm}^{-1}$ ) in lignin were also monitored for their depletion during esterification. Furthermore, acid ( $\text{CH}_2\text{COOH}$  2.20 ppm) conversion to ester ( $\text{CH}_2\text{COO-ester}$  2.30 ppm) could be determined by  $^1\text{H}$  NMR and 56% acid groups were available for the subsequent polycondensation.<sup>36,53</sup> The degree of branching (DB) for a E1 HBP was determined by  $^{13}\text{C}$  NMR and chemical shifts at 53.02, 52.87, and 52.06 ppm were assigned to terminal (*T*), linear (*L*), and dendritic (*D*) structures, respectively as shown in Scheme 2.<sup>21,54</sup> From these assignments and peak intensity the DB could be calculated as 0.711, where

**Table IV.** Tensile Properties of Different Industrial Lignin Based Copolymers at Room Temperature

Sample	Tensile strength (MPa)	Young's modulus (MPa)	Strain at break (%)	Energy at break (MPa)
E1-0	0.40	0.10	259	37
PBE1-20	1.2	2.6	60	40
PBE1-30	2.2	5.4	89	113
PBE1-35	4.9	25.4	77	223
PBE1-40	5.0	12.4	97	282
PBE1-45	15.7	160	89	1020
PBE1-50	16.2	194	58	769
INE1-30	4.2	11.7	70	165
INE1-35	5.7	14.1	114	357
INE1-40	4.2	15.6	107	216
INE1-45	20.8	297	84	1300
CSE1-30	4.2	8.3	86	187
CSE1-35	6.0	7.2	214	634
CSE1-40	3.6	8.4	154	280
CSE1-45	12.6	109	122	1080

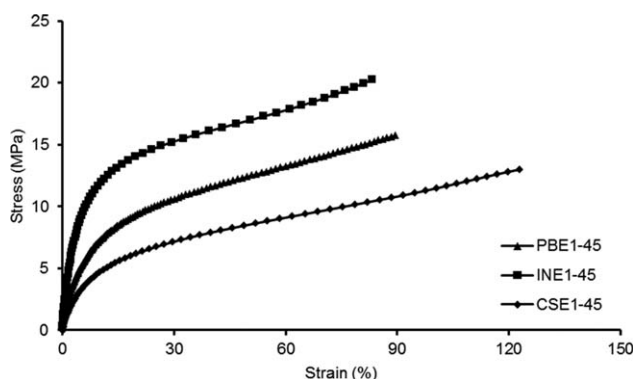


**Figure 4.** Tensile stress-strain curves of PBE1-45, INE1-45 and CSE1-45 copolymers.

$DB = (T + D)/(T + L + D)$ ,<sup>55</sup> The calculated value revealed an appreciably high cross-link occurrence during prepolymerization.  $M_w$  (1206 g/mol) and polydispersity index (1.22) of E1 were determined by ESI-MS (Figure 1 and Table II). Detailed oligomeric composition and sequences based on molecular adduct ions  $[AA_x + TEA_y - H_2O_z + H]^+$  ( $z = x + y - 1$ ) are given in Figure 1 and Table III. Furthermore, detailed analysis of the ESI-MS ions suggests that both acyclic and cyclic structures<sup>56</sup> were present in E1 under the reaction conditions employed. Generally, cyclization could be formed through intramolecular and intermolecular reactions.<sup>54</sup> However, based on ESI-MS, it was exclusively managed to designate the intramolecular reactions (due to side reactions such as intramolecular esterification

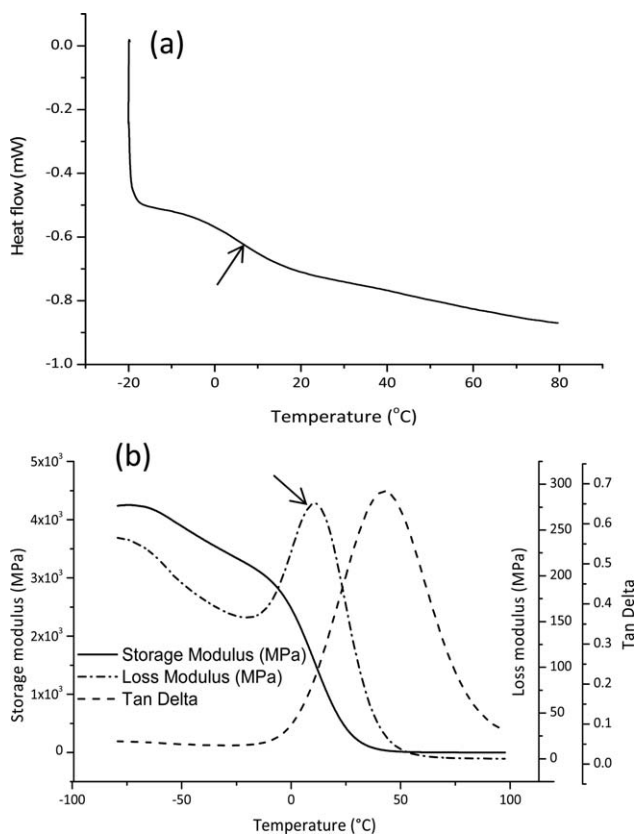


**Figure 5.** DSC (a) and DMA (b) thermograms of PBE1-40 copolymer.

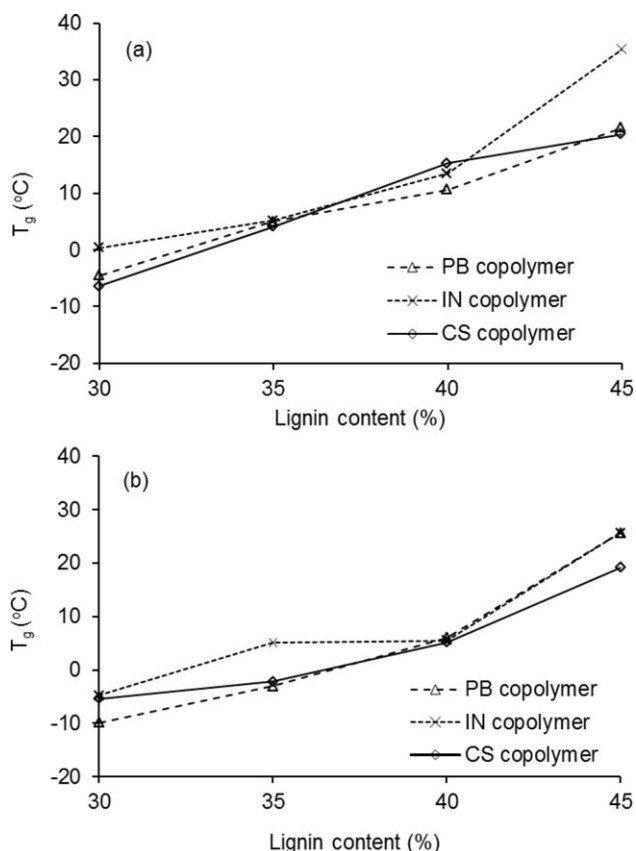


**Figure 6.**  $T_g$  of IN, PB, and CS lignin-copolymers as a function of lignin content, (a) obtained from DMA  $E'$ , and (b) from DSC.

or etherification reactions).<sup>56–58</sup> The representative structures of dimer, trimer and tetramer cyclic structures are illustrated in Scheme 3.

#### Synthesis of Lignin-Copoly(ester-amine) Elastomers

The synthesis route of lignin-copolymer was carried out with a two-step one-pot bulk polymerization (melt condensation) process (Scheme 1).<sup>59</sup> The lignin copolymer formulation was adjusted by using different industrial lignins and lignin content in order to modify lignin-copolymer properties. In the preliminary work, PB lignin with content ranging from 20 to 80%, were used and the final material showed that <30% the lignin-copolymer was too soft to sustain mechanical exertion, while >50% the lignin-copolymer was brittle and showed phase separation. Therefore, for the IN and CS lignin samples, lignin contents evaluated were controlled at 30%, 35%, 40% and 45%. Samples were coded for lignin type (IN, PB, and CS), the HBP E1 and lignin content (20–80%) (e.g. INE1-30) and the control sample without lignin was coded E1-0.

The PBE1-0 to 80 copolymers were analyzed by FT-IR spectroscopy (Figure 2) together with the original PB lignin, acetylated PB lignin, E1-0 control and PBE1-40 copolymer. Ester formation between lignin and HBP was supported by the reduction of the OH band ( $3600\text{--}3100\text{ cm}^{-1}$ ) and increase in the ester carbonyl band ( $1800\text{--}1650\text{ cm}^{-1}$ ). Furthermore, no band at  $1762\text{ cm}^{-1}$  (characteristic of an aromatic carbonyl ester) was observed [Figure 2(d)]. An aliphatic ester band at  $1723\text{ cm}^{-1}$

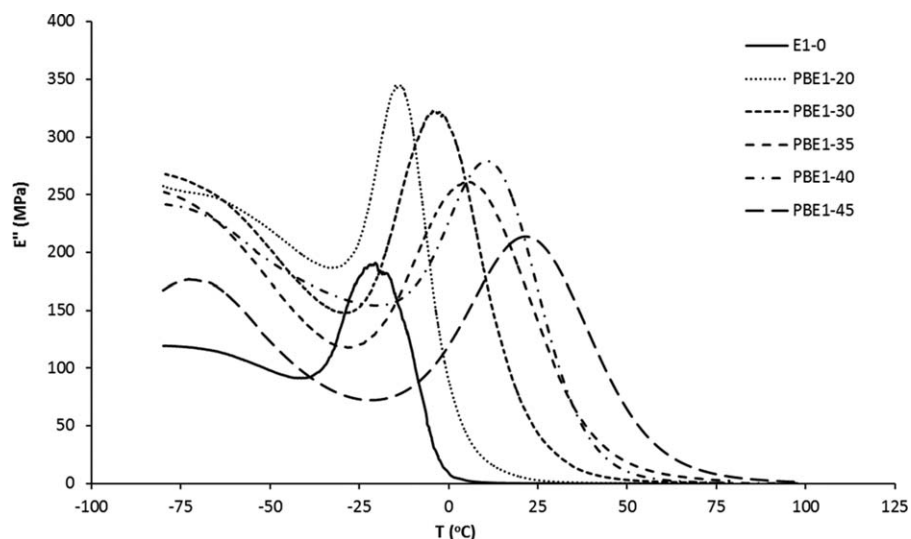


Figure 7. DMA thermograms showing tensile loss moduli ( $E''$ ) for all PBE1-20 to 45 copolymers and E1-0 polymer.

was observed in the copolymer, relative to acetylated lignin (at  $1743\text{ cm}^{-1}$ ), suggesting that aliphatic hydroxyl groups in lignin shows the presence of H-bonding in lignin copolymer.<sup>60</sup> The effect of lignin content on the lignin-E1 copolymer were examined by FT-IR (Figure 3) and showed that the band broadened indicating increased H-bonding with lignin content and this phenomenon has been documented in the literature.<sup>31,60</sup>

### Mechanical Properties

The tensile properties of lignin-copolymers produced are given in Table IV. Stress-strain curves for copolymers INE1-45, PBE1-45 and CSE1-45 are shown in Figure 4. The tensile properties were shown to increase with lignin content to a maximum of 45% lignin content. The control (E1-0) polymer had a tensile strength of 0.4 MPa and increased to 1.2 MPa at 20%

lignin (PBE1-20) and finally to 16.2 MPa at 50% lignin (PBE1-50). The tensile modulus also increased from 0.1 MPa (E1-0 control) to 194 MPa (PBE1-50) as lignin content was increased with a concomitant decrease in strain at break with lignin. The CSE1-30 to 45 and INE1-30 to 45 based copolymers also show similar tensile property trends. There were differences in the tensile properties between the copolymers made with different lignin especially at 45% lignin content. The INE1-45 (20.8 MPa) was shown to have the highest tensile strength followed by PBE1-45 (15.7 MPa) then CSE1-45 (12.6 MPa). A similar trend was observed for the tensile moduli. At high lignin contents the copolymer tensile properties were dominated by lignin and probably due to intramolecular and intermolecular H-bonding. In contrast, at low lignin contents the copolymer tensile properties were dominated by HBP properties and

Table V. Thermal Decomposition of Different Lignin-Based Copolymers from TGA Data

Sample #	1st stage		2nd stage		3rd stage		Max peak
	T (°C)	Remaining mass (%)	T (°C)	Remaining mass (%)	T (°C)	Remaining mass (%)	
PBE1-20	373	78.8	421	28.4	581	16.5	400
PBE1-30	373	77.5	413	35.9	582	22.6	394
PBE1-35	372	80.0	413	40.6	583	25.1	388
PBE1-40	350	84.8	419	35.5	584	25.2	392
PBE1-45	370	81.6	424	43.6	583	29.4	391
PBE1-50	365	82.6	428	43.8	580	30.8	379
INE1-30	375	77.6	418	36.9	566	25.0	391
INE1-35	367	82.7	426	36.3	588	24.2	388
INE1-40	347	86.5	427	36.7	577	26.8	388
INE1-45	374	78.1	424	46.8	557	34.4	387
CSE1-30	377	75.0	417	37.8	554	25.1	394
CSE1-35	357	85.3	418	34.4	566	23.2	395
CSE1-40	359	82.0	413	37.6	564	23.8	389
CSE1-45	364	81.0	421	40.8	564	28.4	388



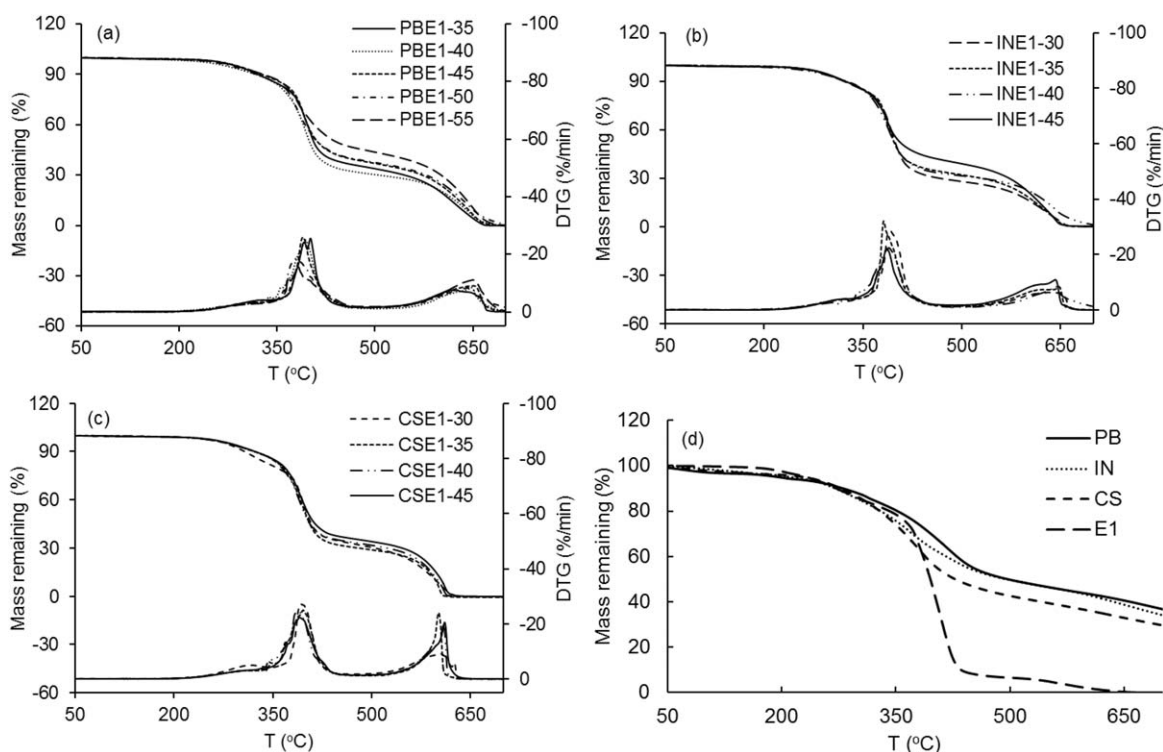


**Figure 8.** TGA thermograms of lignin based copolymers, (a) PB based copolymer, (b) IN based copolymer, (c) CS based copolymer, and (d) starting materials, PB, IN, CS, and E1.

attributable to covalent bonds between HBP and lignin. The toughness of the copolymer was assessed by its energy at break (EAB) and maximum values were obtained at lignin contents of 45%. The EAB of INE1-45, PBE1-45, and CSE1-45 were respectively at 1300, 1020, and 1080 MPa. The data for the lignin-copolymers show that lignin influences the mechanical properties of copolymers.

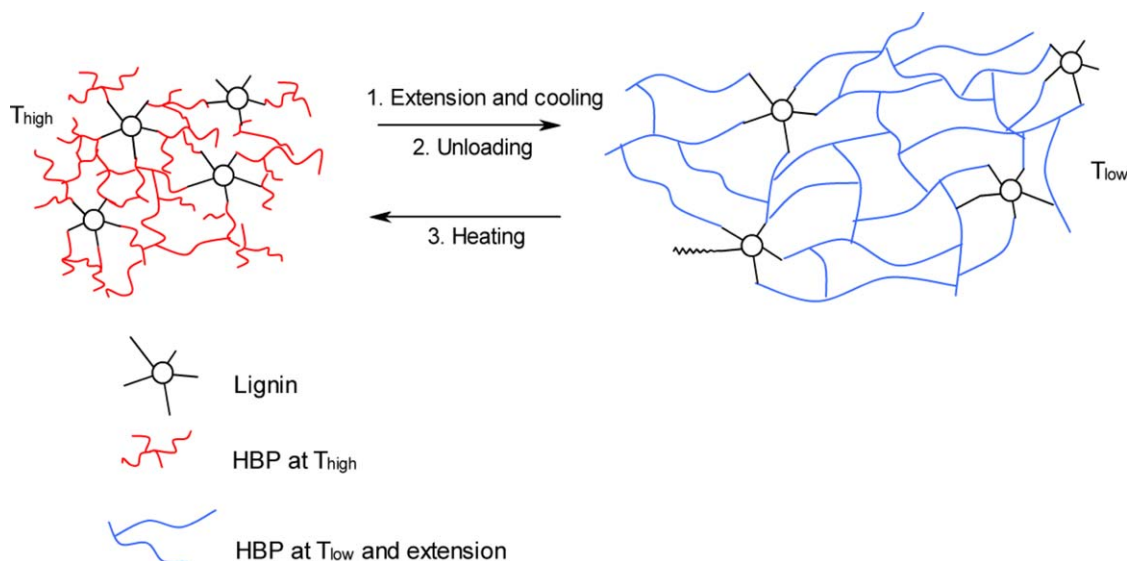
### Thermal Properties

$T_g$  is a second-order phase transition of an amorphous polymeric which confines its threshold in engineering applications.<sup>61</sup> The determination of  $T_g$  of the lignin copolymers was determined by DMA from the maxima of the  $E''$  peak [Figures 5(b) and 6(a)]. In addition,  $T_g$  of the various lignin copolymers were obtained by DSC [Figures 5(a) and 6(b)]. The  $T_g$  was shown to increase with copolymer lignin content. The increasing  $T_g$  of the copolymer could be explained by high  $T_g$  of lignin which introduces an aromatic backbone and H-bonding to the polymer network and as content increases further restricts the free movement of side-chains and reduces the polymer free volume. An interesting point to mention is that the  $T_g$  of IN lignin (117°C) was lower than those of PB (132°C) and CS (131°C), probably due to differences in  $M_w$ , however, the INE1 copolymers showed comparable  $T_g$ s with the other two lignin-copolymers (at a given lignin content). This finding revealed that the E1 HBP plays a determining role in terms of thermal properties and implies that lignin is evenly dispersed in the prepolymer matrix. The miscibility of the two polymers (lignin and E1) was examined by the DSC and DMA. All the DSC thermograms showed one  $T_g$  and the DMA thermograms showed only a single  $E''$

peak for all copolymer samples and this revealed excellent miscibility between the two polymers (Figure 7).<sup>31,60</sup> Miscibility was dependent on the covalent reaction between lignin and E1 and the occurrence of exothermic interactions, such as H-bonding.<sup>38,60</sup> Figure 7 shows that as lignin content increases the  $E''$  peak broadens and lowers in intensity which indicates that increased cross-linking which will result in the reduction of the polymer system volume and thus will require more energy to dissipate the polymer system.<sup>62</sup>

### Thermal Stability of the Lignin-Copoly(ester-amines)

The thermal stability of the lignin-copoly(ester-amines) was studied by TGA. For all copolymers regardless of lignin type, three stages of decomposition were observed by TGA (Table V and Figure 8). To observe the transitions differential TGA (DTG) was also performed (Figure 8). The first stage was between 220 and 350°C. The second stage was between 350 and 425°C. The third stage was between 500 and 650°C. It was reasonable to identify the initial decomposition from E1 and later with from lignin as verified as shown in Figure 8(d), because E1 is constituted with highly branched aliphatic chains and ester groups were considerably labile to thermal decomposition.<sup>63,64</sup> Whereas lignin, comprised of highly cross-linked aromatic backbones and various aliphatic side chains, gradually degraded and resisted thermal decomposition to form appreciable amount of char.<sup>65</sup> Lignin content was not shown to affect the first degradation stage of the copolymers. However, lignin content in the copolymers influenced the second and third stage decompositions [Figure 8(a–c)]. When comparing between copolymers of different lignin type, it appears that IN based copolymers had a



**Scheme 4.** Molecular mechanism of Ts-SME of lignin-co-poly(ester-amine) elastomer. [Color figure can be viewed in the online issue, which is available at [wileyonlinelibrary.com](http://wileyonlinelibrary.com).]

higher relative thermal stability than those made with PB and CS lignin which could be attributed to its more condensed structure (Table V and Figure 8).<sup>28</sup> The residual content for the INE1-45, PBE1-45, and CSE1-45 copolymers at 650°C were respectively, 47%, 44%, and 41%. The variation is contributed by the difference of lignin structure in the higher temperature region.<sup>48</sup>

#### Thermally Stimulated Dual Shape Memory Effect (Ts-SME)

Ts-SME could be obtained in a polymer system which contains two kinds of segments, i.e., soft segment controlling temporary shape and netpoint segment determining permanent shape (Scheme 4).<sup>37</sup> Therefore, this could be applied to the HBP with a flexible aliphatic backbone and side chains having an

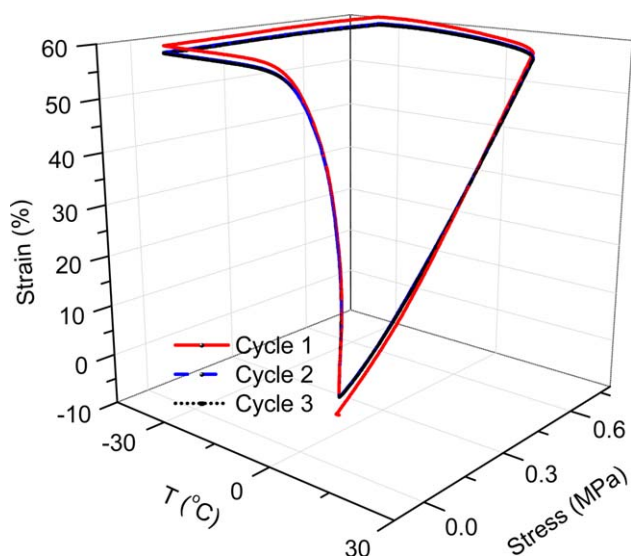


**Figure 9.** Tensile stress-temperature-strain ( $\sigma$ - $T$ - $\varepsilon$ ) curve of PBE1-20 copolymer. [Color figure can be viewed in the online issue, which is available at [wileyonlinelibrary.com](http://wileyonlinelibrary.com).]

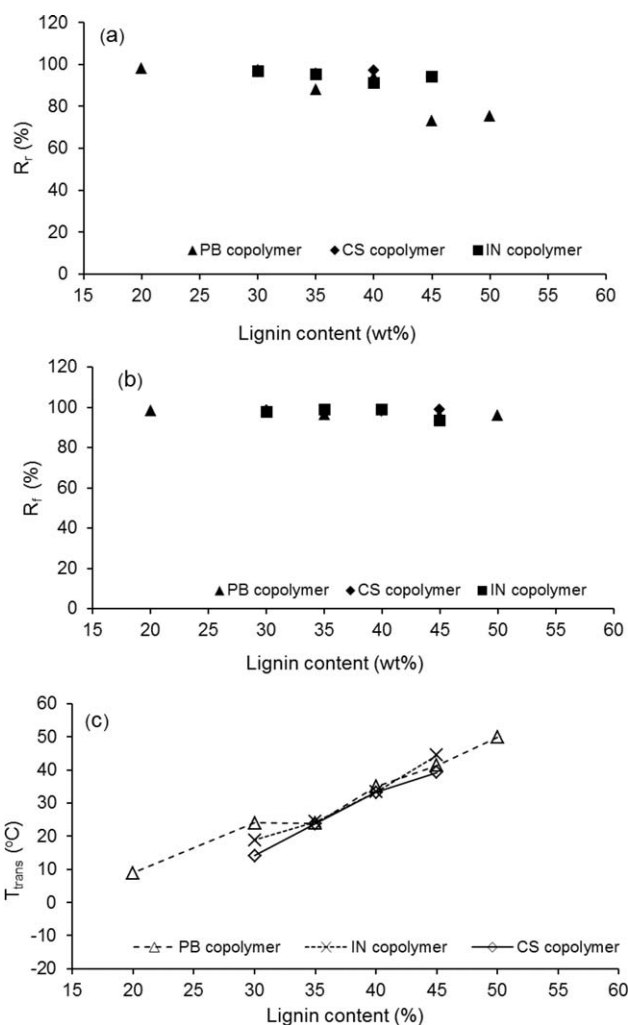


**Figure 10.** (a)  $R_r$ , (b)  $R_p$  and (c)  $T_{trans}$  results of IN, PB and CS lignin-copoly(ester-amines) as a function of lignin content.

appreciably low  $T_g$  and functions as a soft segment. Whereas, lignin is a rigid and compact aromatic structure with a high  $T_g$  and functions as netpoint segment. The SME properties of lignin based copolymers were quantified by tensile stress-controlled thermomechanical cyclic testing. Figure 9 shows the results of cyclic thermomechanical testing of PBE1-20 copolymer. The shape memory recovery ratio ( $R_r$ ) and fixity ratio ( $R_f$ ) were calculated according to the following equations<sup>36</sup>:

$$R_r(N) = \frac{\varepsilon_i(N) - \varepsilon_p(N)}{\varepsilon_i(N) - \varepsilon_p(N-1)} \times 100\% \quad (1)$$

$$R_f(N) = \frac{\varepsilon_u(N)}{\varepsilon_i(N)} \times 100\% \quad (2)$$

where  $R_r(N)$  is the shape recovery ratio at  $N$ th cycle,  $R_f(N)$  is the shape fixity ratio at  $N$ th cycle,  $N$  is cycle number from 1 to 3,  $\varepsilon_i(N)$  is the maximum strain with load,  $\varepsilon_u(N)$  is the tensile strain after unloading at  $T_{low}$ ,  $\varepsilon_p(N-1)$ , and  $\varepsilon_p(N)$  are the recovered strain in two successive cycles in the stress-free state before exertion of yield stress at  $T_{high}$ . Reporting values were based on the average of three cycles. Second and third cycles were highly superimposable and overlapped compared to the first cycle and an appreciable improvement of  $R_f$  and  $R_r$  observed. This small training effect was contributed by the occurrence of some chain relaxation during the first mechanical cycle, leading to a deviation in the later cycles, which was a characteristic phenomenon of SMPs according to Gautrot and Zhu.<sup>66,67</sup>  $R_f$  describes the ability to fix the mechanical deformation under  $T_{low}$ , while  $R_r$  quantifies how well the shape recovers in the  $N$ th cycle (for  $N > 1$ ) in terms of the recovered shape of the previous ( $N - 1$ )th cycle.<sup>67,68</sup> The results of  $R_r$  and  $R_f$  of all the lignin copoly(ester-amines) as a function of lignin content are shown in Figure 10(a,b), respectively. All the copolymers were shown to have high  $R_f$  with more than 95% fixity rate. The PB based copolymers were shown to have an excellent  $R_r > 85\%$  at lignin contents  $< 40\%$ . However, at lignin content greater than 40%, the  $R_r$  values decreased to 73% for PBE1-45 and 76% for PBE1-50. A 90% shape recovery was obtained for all the CS and IN based copolymers.  $T_{trans}$  is another important parameter of Ts-SME polymers and was determined at which the polymer can be switched back to its original shape upon removal of external stimuli measured as first derivative peak of the strain versus temperature plot. The  $T_{trans}$  of various lignin-copolymers as a function of lignin content is shown in Figure 10(c). It was observed that the  $T_{trans}$  increased for the lignin-copoly(ester-amines) with lignin content implying that this parameter could be tailored to meet specific temperature requirements.  $T_{trans}$  was approximately 20°C higher than the  $T_g$  of the copolymers (determined from  $E'$ ). The  $T_{trans}$  of the different lignin based copolymers were comparable at the same lignin content, which indicated that the  $T_{trans}$  of the copolymers was dominated by the soft segment.

## CONCLUSIONS

Lignin-based Ts-SME dual shape memory copolymers were successfully synthesized using a variety of industrial lignins and HBP via a one-pot two step bulk polycondensation reaction. Lignin content and lignin type (IN, PB, and CS) were shown to influence copolymer properties. At high lignin levels ( $> 40\%$ )

the copolymer mechanical properties were dominated by lignin while  $\leq 40\%$  lignin the properties were dominated by HBP. The copolymers were shown to have  $> 95\%$  fixity rate and  $> 90\%$  shape recovery. The  $T_{trans}$  was shown to increase with copolymer lignin content and this demonstrates that the properties can be tuned by lignin content. This study clearly demonstrates that lignin, a renewable resource and byproduct, can be used as a netpoint segment in polymer systems with SME behavior.

## ACKNOWLEDGMENTS

The authors acknowledge (i) the financial support from a USDA-NIFA Wood Utilization Research grant number 2010-34158-20938, (ii) Dr. Alexander Blumenfeld for his technical help with NMR, (iii) USDA-CSREES grants 2007-34158-17640 and 2005-35103-15243 for supporting the DSC/DMA and FT-IR spectrometer, respectively, and (iv) Thermoscientific for the LCQ-Deca mass spectrometer.

## REFERENCES

- Chung, H.; Washburn, N. R. *Green Mater.* **2013**, *1*, 137.
- Teramoto, N. In *A Handbook of Applied Biopolymer Technology: Synthesis, Degradation and Applications*; Sharma, S. K., Mudhoo, A., Eds.; Royal Society of Chemistry, London, **2011**; Chapter 2, p 22.
- Drumright, R. E.; Gruber, P. R.; Henton, D. E. *Adv. Mater.* **2000**, *12*, 1841.
- Proiakakis, C. S.; Tarantili, P. A.; Andreopoulos, A. G. *J. Elastomers Plast.* **2002**, *34*, 49.
- Kawashima, N. *J. Synth. Org. Chem Jpn.* **2003**, *61*, 496.
- Kawashima, N.; Matsuo, M.; Sugi, M. *Kobunshi Ronbunshu* **2005**, *62*, 233.
- El Idrissi, A.; El Barkany, S.; Amhamdi, H.; Maaroufi, A. K. *J. Appl. Polym. Sci.* **2013**, *127*, 3633.
- Beheshti, N.; Nguyen, G. T. M.; Kjoniksen, A. L.; Knudsen, K. D.; Nystrom, B. *Colloids Surf. A* **2006**, *279*, 40.
- Hu, S. J.; McDonald, A. G.; Coats, E. R. *J. Appl. Polym. Sci.* **2013**, *129*, 1314.
- Wei, L.; Guho, N. M.; Coats, E. R.; McDonald, A. G. *J. Appl. Polym. Sci.* **2014**, *131*, 40333.
- Boonprasith, P.; Wootthikanokkhan, J.; Nimitsiriwat, N. *J. Appl. Polym. Sci.* **2013**, *130*, 1114.
- Pang, M. M.; Pun, M. Y.; Ishak, Z. A. M. *J. Appl. Polym. Sci.* **2013**, *129*, 3237.
- Quirino, R. L.; Garrison, T. F.; Kessler, M. R. *Green Chem.* **2014**, *1700*.
- Valverde, M.; Yoon, S.; Bhuyan, S.; Larock, R. C.; Kessler, M. R.; Sundararajan, S. *Macromol. Mater. Eng.* **2011**, *296*, 444.
- Miao, S. D.; Wang, P.; Su, Z. G.; Liu, Y. Y.; Zhang, S. P. *Eur. J. Lipid Sci. Technol.* **2012**, *114*, 1345.
- Perlack, R. D.; Wright, L. L.; Turhollow, A.; Graham, R. L.; Stokes, B. J.; Erbach, D. C. *Biomass as Feedstock for a Bioenergy and Bioproducts Industry: The Technical Feasibility of a*

- Billion-Ton Annual Supply. *Tech. Rep.* DOE/GO-102005-2135. Oakridge, Oak Ridge National Laboratory. **2005**.
17. Lewis, N. G.; Lantzy, T. R. In *Adhesive from Renewable Resources*; Hemingway, R. W., Conner, A. H., Branham, S. J., Eds.; ACS Symposium Series: New Orleans, **1989**; p 13.
  18. Zakzeski, J.; Bruijninx, P. C. A.; Jongerius, A. L.; Weckhuysen, B. M. *Chem. Rev.* **2010**, *110*, 3552.
  19. Gosselink, R. J. A.; de Jong, E.; Guran, B.; Abächerli, A. *Ind. Crop Prod.* **2004**, *20*, 121.
  20. Li, Y.; Mlynar, J.; Sarkanen, S. *J. Polym. Sci., Part B: Polym. Phys.* **1997**, *35*, 1899.
  21. Sivasankarapillai, G.; McDonald, A. G.; Li, H. *Biomass Bioenergy.* **2012**, *47*, 99.
  22. Li, Y.; Sarkanen, S. *Macromolecules* **2002**, *35*, 9707.
  23. McDonald, A. G.; Ma, L. In *Lignin: Properties and Applications in Biotechnology and Bioenergy*; Paterson, R. J., Ed.; Nova Science Publisher, Inc., New York, **2012**; Chapter 19, p 489.
  24. Cui, C. Z.; Sadeghifar, H.; Sen, S.; Argyropoulos, D. S. *Bio-Resources* **2013**, *8*, 864.
  25. Sadeghifar, H.; Cui, C.; Argyropoulos, D. S. *Ind. Eng. Chem. Res.* **2012**, *51*, 16713.
  26. Wu, L. C. F.; Glasser, W. G. *J. Appl. Polym. Sci.* **1984**, *29*, 1111.
  27. Li, Y.; Ragauskas, A. J. *J. Wood Chem. Technol.* **2012**, *32*, 210.
  28. Glasser, W. G.; Jain, R. K. *Holzforchung* **1993**, *47*, 225.
  29. Fox, C. S.; McDonald, A. G. *BioResources.* **2010**, *5*, 990.
  30. Saito, T.; Brown, R. H.; Hunt, M. A.; Pickel, D. L.; Pickel, J. M.; Messman, J. M.; Baker, F. S.; Keller, M.; Naskar, A. K. *Green Chem.* **2012**, *14*, 3295.
  31. Sivasankarapillai, G.; McDonald, A. G. *Biomass Bioenergy.* **2011**, *35*, 919.
  32. Li, H.; Sivasankarapillai, G.; McDonald, A. G. *J. Appl. Polym. Sci.*, **2014**, DOI: 10.1002/app.41103.
  33. Sailaja, R. R. N.; Deepthi, M. V. *Mater. Design* **2010**, *331*, 4360.
  34. Pohjanlehto, H.; Setälä, H. M.; Kiely, D. E.; McDonald, A. G. *J. Appl. Polym. Sci.* **2014**, *131*, 39714.
  35. Laurichesse, S.; Avérous, L. *Prog. Polym. Sci.* **2014**, *39*, 1266.
  36. Kim, Y. S.; Kadla, J. F. *Biomacromolecules.* **2010**, *11*, 981.
  37. Lendlein, A.; Kelch, S. *Angew. Chem. Int. Ed.* **2002**, *41*, 2034.
  38. Xie, T. *Nature* **2010**, *464*, 267.
  39. Behl, M.; Lendlein, A. *Mater. Today* **2007**, *10*, 20.
  40. Lendlein, A.; Langer, R. *Science* **2002**, *296*, 1673.
  41. Liu, C.; Qin, H.; Mather, P. T. *J. Mater. Chem.* **2007**, *17*, 1543.
  42. Beloshenko, V. A.; Beigelzimer, Y. E.; Varyukhin, V. N.; Voznyak, Y. V. *Polym. Sci. Ser. A* **2005**, *47*, 723.
  43. Yakacki, C. M. *Polym. Rev.* **2013**, *53*, 1.
  44. Behl, M.; Lendlein, A. In *Shape-Memory Polymers and Multifunctional Composites*; Leng, J. S., Du, S. Y., Eds.; CRC Press: Boca Raton, **2010**; p 1.
  45. Xie, T. *Polymer* **2011**, *52*, 4985.
  46. Dietsch, B.; Tong, T. J. *Adv. Mater.* **2007**, *39*, 3.
  47. Wagermaier, W.; Kratz, K.; Heuchel, M.; Lendlein, A. In *Shape-Memory Polymers*; Lendlein, A., Ed.; Springer-Verlag: Berlin, **2010**; p 97.
  48. Li, H. *Synthesis and Characterization of Copolymers from Lignin*. Ph.D. Dissertation, University of Idaho: Moscow, Idaho, **2014**.
  49. Capanema, E. A.; Balakshin, M. Y.; Kadla, J. F. *J. Agric. Food. Chem.* **2004**, *52*, 1850.
  50. Osman, N. B.; McDonald, A. G.; Laborie, M. P. G. *Holzforchung* **2012**, *66*, 927.
  51. Parees, D. M.; Hanton, S. D.; Clark, P. A. C.; Willcox, D. A. *J. Am. Soc. Mass. Spectrom.* **1998**, *9*, 282.
  52. Teng, N.-Y.; Dallmeyer, I.; Kadla, J. F. *Ind. Eng. Chem. Res.* **2013**, *52*, 6311.
  53. Stumbe, J. F.; Bruchmann, B. *Macromol. Rapid Commun.* **2004**, *25*, 921.
  54. Holter, D.; Burgath, A.; Frey, H. *Acta Polym.* **1997**, *48*, 30.
  55. Hawker, C. J.; Lee, R.; Frechet, J. M. J. *J. Am. Chem. Soc.* **1991**, *113*, 4583.
  56. Li, X.; Lu, X.; Lin, Y.; Zhan, J.; Li, Y.; Liu, Z.; Chen, X.; Liu, S. *Macromolecules.* **2006**, *39*, 7889.
  57. Voit, B. I.; Lederer, A. *Chem. Rev.* **2009**, *109*, 5924.
  58. Kricheldorf, H. R. *Macromol. Rapid Commun.* **2007**, *28*, 1839.
  59. Scholl, M.; Nguyen, T. Q.; Bruchmann, B.; Klok, H. A. *Macromolecules* **2007**, *40*, 5726.
  60. Kadla, J. F.; Kubo, S. *Macromolecules* **2003**, *36*, 7803.
  61. Overley, R. M.; Buenviaje, C.; Luginuni, R.; Dinelli, F. *J. Therm. Anal. Calorim.* **2000**, *59*, 205.
  62. del Río, E.; Lligadas, G.; Ronda, J. C.; Galià, M.; Cádiz, V.; Meier, M. A. R. *Macromol. Chem. Phys.* **2011**, *212*, 1392.
  63. Pramanik, S.; Konwarh, R.; Sagar, K.; Konwar, B. K.; Karak, N. *Prog. Org. Coat.* **2013**, *76*, 689.
  64. Pramanik, S.; Konwarh, R.; Barua, N.; Buragohain, A. K.; Karak, N. *Biomater. Sci.* **2014**, *2*, 192.
  65. Nassar, M. M.; MacKay, G. D. M. *Wood Fiber Sci.* **1984**, *16*, 441.
  66. Gautrot, J. E.; Zhu, X. X. *Macromolecules* **2009**, *42*, 7324.
  67. Gautrot, J. E.; Zhu, X. X. *Angew. Chem. Int. Ed.* **2006**, *45*, 6872.
  68. Sauter, T.; Heuchel, M.; Kratz, K.; Lendlein, A. *Polym. Rev.* **2013**, *53*, 6.